ChemComm

Rational ligand choice extends the SABRE substrate scope

Journal:	*ChemComm*
Manuscript ID	CC-COM-02-2020-001330
Article Type:	Feature Article

Journal Name

ARTICLE

Rational ligand choice extends the SABRE substrate scope

Johannes F. P. Colell[a‡], Angus W. J. Logan[a‡], Zijian Zhou[a], Jacob R. Lindale[a], Raul Laasner[b], Roman V. Shchepin[c], Eduard Y. Chekmenev[d,e], Volker Blum[a,b], Warren S. Warren[a,f]*, Steven J. Malcolmson[a]* and Thomas Theis[a,g,h]*

Received 00th January 20xx,
Accepted 00th January 20xx

DOI: 10.1039/x0xx00000x

www.rsc.org/

Signal Amplification By Reversible Exchange (SABRE) is a particularly simple hyperpolarisation approach. However, compared to other hyperpolarisation methods, SABRE is more limited in substrate scope. Therefore, it is critical to understand and overcome the factors limiting generalization. Past developments in SABRE catalyst optimization have emphasized large enhancements in the canonical SABRE substrate: pyridine and structurally closely related motifs. However, the pyridine-optimized catalysts are not efficient at hyperpolarising more sterically demanding substrates, including 2-substituted pyridine derivatives. Here we report that modifications of the catalyst ligand sphere, using a chelating ligand in particular, can increase the volume fraction available for substrate coordination to the iridium catalyst, thus permitting significant signal enhancements on otherwise sterically hindered substrates. The system yields ^{1}H enhancements on the order of 100-fold over 8.5 T thermal measurements for 2-substituted pyridine derivatives, and smaller, yet significant ^{1}H enhancement for provitamin B_6 and caffeine. For the 2-substituted pyridine derivatives we further show ^{15}N enhancements on the order of 1000-fold and ^{19}F enhancements of 30-fold over 8.5 T thermal polarisations.

Introduction

Signal Amplification By Reversible Exchange (SABRE) is a relatively recent discovery among hyperpolarisation methods (2009).[1-5] Hyperpolarisation is transferred from *para*-hydrogen (*p*-H_2) to nuclei in a substrate molecule through *J*-coupling interactions mediated by the metal centre of a polarisation transfer catalyst. Both parahydrogen and substrate are in reversible exchange on the catalyst and polarisation flows from parahydrogen derived hydrides[6] to ligated substrates during the lifetime of the complex. [1, 7]

SABRE is an attractive hyperpolarisation technique because it allows for efficient polarisation of ^{1}H and ^{15}N spins within about one minute.[8-10] The technique uses simple and low-cost hardware and has been expanded to a wide range of other spin-1/2 nuclei including ^{13}C, ^{19}F, ^{31}P, and others[5, 11-16] Moreover, heterogeneous SABRE and SABRE in aqueous medium have been demonstrated.[17-27] All-in-all, this technique has made large advances for preparation of hyperpolarised substances, and has demonstrated the potential to generate injectable hyperpolarised contrast agents for *in vivo* magnetic resonance spectroscopic imaging.[28-32,33]

In this paper, we capitalize on the simple insight that steric considerations are of essence and can make a drastic difference in SABRE efficiency. Particularly, substrate size and binding pocket must be well matched. Guided by this insight, we introduce a hyperpolarisation catalyst able to hyperpolarise larger, sterically hindered substrates, primarily 2-substituted pyridines, that are not efficiently hyperpolarised with current widely used catalysts.[10, 34] Moreover, we demonstrate hyperpolarisation of provitamin B_6 and caffeine, which bear substituents in the ortho position to the N-heteroatom as well.

Historically, SABRE was discovered with Crabtree's catalyst [Ir(PR_3)(pyr)(COD)]PF_6 (**1**) (R = cyclohexyl, pyr = pyridine, COD = 1,5-cyclooctadiene) (**see Figure 1**)[1]. Initially, ^{1}H signal amplifications over thermal signals (enhancements) were found to scale favourably with electron density and steric bulk of the phosphine ligand[2], but phosphine ligands were quickly replaced by N-heterocyclic carbenes (NHCs), most importantly, IMes[35] **(2)** and **(2a) (Figs. 1 and 2,** IMes = 1,3-bis(2,4,6-trimethylphenyl)imidazole-2-ylidene)**),** giving rise to a drastic increase of enhancements.[35-37]

[a] Department of Chemistry, Duke University, Durham, NC 27708, USA.
[b] Department of Mechanical Engineering and Materials Science, Duke University, Durham, NC 27708, USA.
[c] Department of Chemistry, Biology, and Health Sciences, South Dakota School of Mines and Technology, Rapid City, South Dakota 57701, USA
[d] Russian Academy of Sciences, Leninskiy Prospekt 14, 119991 Moscow, Russia.
[e] Department of Chemistry, Integrative Biosciences (IBio), Karmanos Cancer Institute (KCI), Wayne State University, Detroit, MI 48202, USA.
[f] Departments of Physics, Radiology and Biomedical Engineering, Duke University, Durham, NC 27707, USA.
[g] Department of Chemistry, North Carolina State University, Raleigh, NC 27695
[h] Joint Department of Biomedical Engineering University of North Carolina at Chapel Hill and North Carolina State University, Chapel Hill, NC, USA
‡ These authors contributed equally.
Corresponding Authors
Steven J. Malcolmson, steven.malcolmson@duke.edu
Warren Warren, warren.warren@duke.edu
Thomas Theis, ttheis@ncsu.edu
Electronic Supplementary Information (ESI) available: Synthesis of the catalyst, detailed DFT calculations, spectral data, magnetic evolution field dependence, and description of experimental details. See DOI: 10.1039/x0xx00000x

Most optimization efforts using the NHC motif were geared towards pyridine and structurally similar compounds.[38, 39] Large improvements for ^{1}H SABRE were recently afforded with perdeuterated[8] or chlorinated [40] variant of the [IrCl(IMes)(COD)] (**2**) system with record polarisations on the order of 50%. However, these improvements do not extend to other substrates with higher steric demands. In efforts to target a broader substrate scope, auxiliary compounds (co-ligands) have been utilized to increase the number of viable polarisation transfer targets and to focus transferred polarisation.[16, 41-44] Also, chelating ligands have been explored, but polarisation levels remained low. [45, 46] While a variety of smaller pyrazole derivatives were studied in Ref.[47], polarisation on 2-substituted pyridines was not reported.

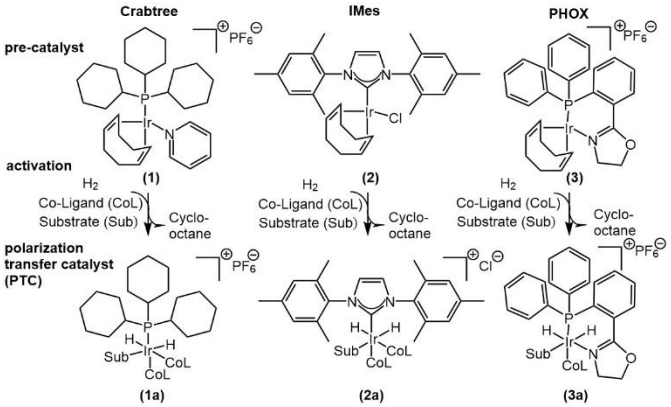

Figure 1: Three generations of catalysts for SABRE. The canonical Crabtree's catalyst (**1**), the IMes catalyst (**2**) yielding maximal enhancements on pyridine, and the Phox catalyst (**3**) applicable to sterically demanding substrates, as shown here. Coligands (CoL) are constituted by solvent, substrate or an auxiliary compound.

Here we demonstrate that [Ir(COD)(Phox)]PF_6 (**3**) (Phox = 2-(2-(diphenylphosphanyl)phenyl)-4,5-dihydrooxazole) (Figure 1), a catalyst for asymmetric hydrogenation of olefins[48], can serve as a polarisation transfer catalyst for more sterically demanding substrates.[49, 50] We target ^{1}H, ^{15}N and ^{19}F hyperpolarisation in ortho-substituted pyridine derivatives, including provitamin B_6 and caffeine. It is noteworthy, that although **(3)** performs *worse* as a polarisation transfer catalyst for pyridine, compared to **(2)**, it is superior for sterically congested substrates, which are not hyperpolarised with the IMes catalyst **(2)** at all.

As illustrated in Figure 1, in SABRE experiments, precatalysts are transformed into their catalytically active species under a H_2 atmosphere in presence of polarisation transfer targets. For precatalyst (**2**) and the substrate pyridine, one obtains $[Ir(H)_2(IMes)(pyr)_3]^+$ (**2a**). This dihydride derived from *p*-H_2 constitutes the catalytically active complex in polarisation transfer reactions.[35, 51] One important consequence of monodentate ligands (e.g. an NHC or Phosphines) and the octahedral iridium dihydride complexes is that three sites remain for coordination (pyridine in **(2a)**). By using a bidentate ligand, such as [Ir(COD)(Phox)]PF_6 **(3)** the binding pocket size is significantly increased over that of complexes with monodentate ligands.

When pre-catalyst **(3)** is activated under a hydrogen atmosphere in the presence of substrates, **(3a)** is formed (see Fig. 1 and 2A). Evidence for (3a) is provided by NMR data (Fig. 2B and see below) and accompanying density-functional theory (DFT) calculations.[52-56] The DFT code used (FHI-aims[52, 57, 58]) is a high-precision, all-electron implementation that has been benchmarked extensively in past work,[59, 60] including a history of successful use for molecular structure prediction (e.g., Refs.[61-64]). Detailed analysis of the DFT calculations, including extensive benchmark and validation data for the methods used, is presented in the Supporting Information. The DFT calculations find **(3a)** to be the lowest energy dihydride complex. Consistent with this structure, we find different chemical shifts for the two hydride species attached to Ir, as displayed in Fig. 2. Specifically, if *para*-hydrogen is bubbled through the solution at high field (8.45 T) the anti-phase spectrum of Figure 2B is obtained. [65, 66] We observe chemical shifts of -19.0 and -22.5 ppm for the hydride resonances, pointing to trans-to nitrogen coordination for both hydrides, where the chemical shift at -22.5 ppm is identical with the *trans*-to-pyridine hydride in **(2a)**.

The observed hydride to hydride *J*-coupling in **(3a)** is $J_{HH'} \approx -7$ Hz and the hydride to ^{31}P *J*-couplings are $J_{HP} = J_{H'P} \approx 20$ Hz. The *J*-couplings, chemical shifts, and magnetic field dependence of hyperpolarisation (see supplement) are very similar to those of

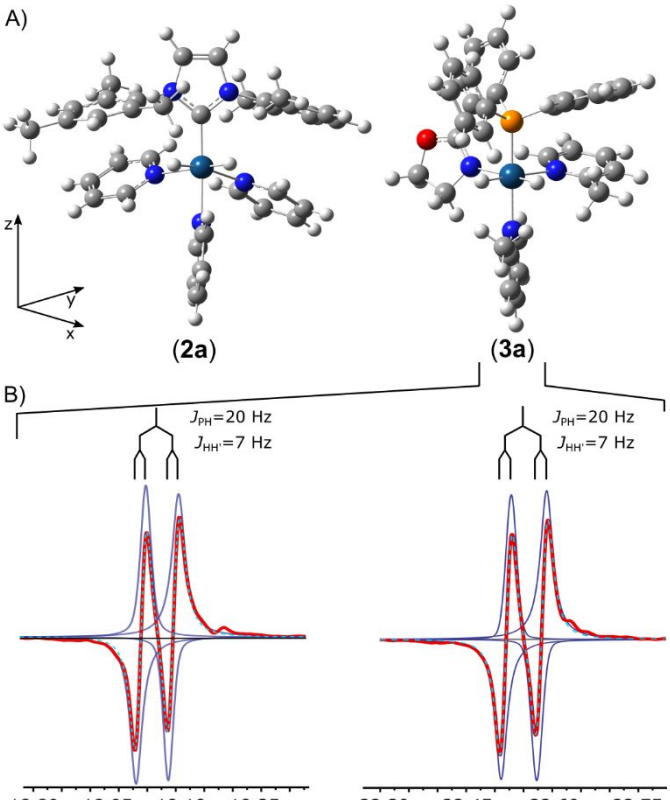

Figure 2: A) Comparison of the structure of $[Ir(H)_2(IMes)(pyr)_3]^+$ (**2a**) and the structure predicted for $[Ir(H)_2(Phox)(MP)_2]^+$ (**3a**) (MP = 2-methylpyridine). B) Experimental Spectrum (red) and fit (dashed line, cyan) of the hydride resonances of (**3a**). For the experiment, constant *para*-H_2 flow was supplied at 8.45 T and the excitation pulse is 45°. The fit is the sum of individual resonances (blue curves). The maxima of the blue curves can be used to extract δ = -19.03 and -22.55 ppm, using $J_{HH'} \approx -7$ Hz, $J_{HP} = J_{H'P} \approx 20$ Hz as shown in the small insets directly above the spectra. With a chemical shift difference of approximately 3.5 ppm, a PASADENA-like spectrum is obtained.

Crabtree's catalyst, serving as further evidence for structure **(3a)**. While a full conformational study of **(3a)** at relatively low concentrations remains beyond the scope of this work, the proposed structure **(3a)** provides a consistent mechanistic explanation for the main observation of this paper, which is the ability of **(3)** and its activated state to successfully hyperpolarize substrates that are much more difficult to access with other commonly used catalysts.

We found that **(3)** allows ^{1}H polarisation in a range of 2-substituted pyridines, where the conventional IMes catalyst **(2)** is not applicable. Table 1 contrasts ^{1}H enhancements obtained with the first-generation Crabtree's catalyst **(1)**, the IMes catalyst **(2)** optimized for pyridine, and the bidentate Phox catalyst **(3)**. As in studies using **(1)**, maximum enhancements on substrate ^{1}H nuclei with **(3)** are obtained at 140 G irrespective of substrate identity (see SI). This is consistent with the study of Pravdivtsev *et al.*, where presence of ^{31}P in the first coordination sphere of Ir changes the matching conditions to a higher magnetic field when compared to **(2)**.[67] It is noteworthy that catalyst **(3)** yields enhancements of aromatic protons in α-picoline and 2-fluoropyridine (Table 1, entries 2 and 3), comparable to those originally reported for SABRE with Crabtree's catalyst **(1)** and pyridine (Table 1, entry 1).[1, 2] Interestingly, Crabtree's catalyst yields a small but non-negligible hyperpolarisation effect on 2-fluoropyridine in that the sign of the polarisation changed compared to simple thermal polarisation. This shows that the activity of Crabtree's catalysts is not strictly zero for this substrate but still drastically lower than that of the Phox catalyst **(3)**. Similar small but non-zero activity is possible for the other cases labeled "-" in Table 1, however, remained below the detection limits of our experiments.

Table 1: Comparison of average ^{1}H enhancements ε at RT (over thermal signals at 8.5 T). Asterisks in the molecular sketches denote the enhanced ^{1}H moieties. No enhancements are observed for substrate 6.

Entry	substrate name	structure	^{1}H ε with Crabtree **(1)**	^{1}H ε with IMes **(2)**	^{1}H ε with Phox **(3)** aromatic/ aliphatic
1	pyridine		100	1300	2
2	α-picoline		–	–	132/11
3	2-fluoro-pyridine		1[a]	–[b]	140
4	2-ethyl-pyridine	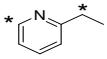	–	–	25/5
5	provitamin B_6	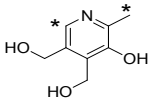	–[c]	–[c]	7/2[c]
6	2,6-lutidine		–	–	–
7	caffeine	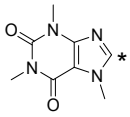	–	–	4[d]

a) Non-thermal signal (negative sign relative to thermal reference) but identical integral observed. b) HD exchange of 2-fluoropyridine with solvent observed, see Fig. S16 in SI. c) From pyridoxine*HCl (neutralized with NaOD 40 wt% in D_2O).
d) Saturated in MeOH-d_4 (23 mM); only aromatic H enhanced.

The enhancements for aliphatic proton are relatively poor for all entries (~10-fold). Comparing entries 2 and 4, increasing the chain length of the aliphatic substituent reduces aromatic proton enhancements by 80%. Potentially the most interesting structure, from an application viewpoint, is provitamin B_6 (entry 5). In our experiments, enhancements of aromatic and aliphatic protons of 7 and 2 respectively were achieved. The enhancements were limited since the provitamin B6 was commercially available only as a hydrochloride salt, which necessitated addition of a base (triethylamine or NaOD) for neutralization. This procedure also resulted in addition of a small amount of water, which reduces SABRE efficiency somewhat. Regarding the limitations by sterical congestion, we note that hyperpolarisation of 2,6-dimethylpyridine (entry 6) remained unsuccessful. To rationalize this finding, we show in the supplement (Figure S5, Table S9, as well as an analysis of strain effects in Supplemental section 2d and Tables S10-S13) that DFT modelling of the substitution of 2-methylpyridine (entry 2) in **(3a)** by 2,6-dimethylpyridine results in an approximate energy increase of +0.5 eV (48 kJ/mol), much larger than $N_a k_B T$. Adding additional co-ligands (CH_3CN, H_2O, Pyridine), an approach that was successful in prior instances with sterically hindered substrates,[10, 16, 41, 43, 68] also failed to effect hyperpolarisation of 2,6-dimethylpyridine in the present work. Entries 1 (pyridine) and 7 (caffeine) show small but non-zero enhancements. For caffeine (entry 7), small enhancements are expected as caffeine is the largest substrate we examined and may require a catalyst optimized for even larger motifs.

Next, we used the Phox catalyst **(3)** for polarising ^{15}N at μT magnetic fields with SABRE-SHEATH.[7, 10, 17, 69-71] The simple substrate CH_3CN has previously been found to show 190-fold ^{1}H polarisation enhancements when used as a coligand with the IMes catalyst.[72] We investigated ^{15}N polarisation with $CH_3C^{15}N$ (50 mM) and 2.6 mM solutions of **(3)** as a function of temperature at microTesla fields as displayed in Fig. 3. We found that ^{15}N polarisation levels of 1.5 % are readily obtained, identical to polarisation levels achieved with **(2)** at these moderately high concentrations.[10] As indicated in Fig. 3, the optimal temperature is elevated when using the Phox catalyst **(3)**. Here the maximum is found between 60 °C and 70 °C, whereas IMes works best at room temperature for ^{15}N-acetonitrile **(2)**.[10] Next, as shown in the bottom of Fig. 3, the Phox catalyst **(3)** hyperpolarises ^{15}N at natural abundance in substrates 1-4 using 2.6 mM catalyst and 50 mM substrate (see Fig. 3, bottom). Notice that the nitrogen enhancements ε are larger for ^{15}N than for ^{1}H. However, the absolute polarisation levels are similar because the enhancement refers to thermal polarisation of ^{15}N, which is ten times lower than for ^{1}H. We also note that similar temperature dependent measurements were not possible for ^{1}H with our present

setup since ^{1}H relaxation times are shorter, leading to larger uncertainties as a result of having to transfer samples manually between a temperature controlled mT field environment and the spectrometer.

Finally, we also tested the previously challenging[12] ^{19}F

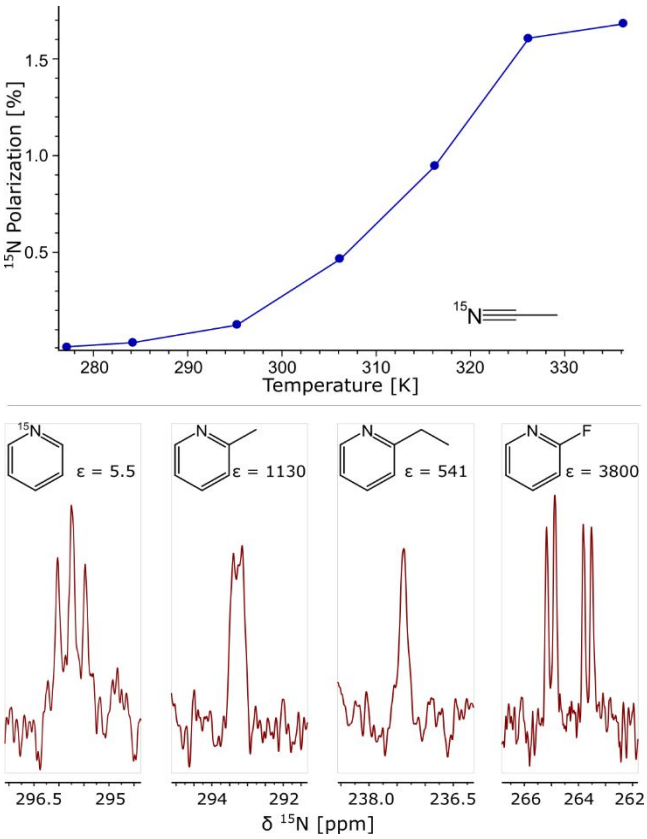

Figure 3: (Top) ^{15}N Polarisation with PHOX **(3)** as a function of the sample temperature during polarisation build-up on ^{15}N labelled CH_3CN in the magnetic shield. Evolution field is 0.66 μT, build-up time 60 s. (Bottom) ^{15}N spectra of naturally abundant 2-substituted pyridine derivatives and ^{15}N labelled pyridine hyperpolarised by SABRE-SHEATH at room temperature. 2.6 mM catalyst (3) and 50 mM substrate were used in all samples.

polarisation of 2-fluoropyridine (i.e., ^{19}F in the ortho position) and achieved a 30-fold enhancement over thermal polarisation at 9.4 T, at an optimised polarisation transfer field of 5.4 mT (Figure S15 in the supplement). In Ref.[12], it was shown that ^{19}F in the ortho position was difficult to hyperpolarize with the IMes catalyst (attributed to steric hindrance) whereas here we achieve hyperpolarisation with the Phox catalyst.

In conclusion, the introduced PHOX multidentate ligand for SABRE catalysts allows for polarisation of bulkier substrates, including biologically relevant molecules such as provitamin B_6 or caffeine. Interestingly, hyperpolarisation is worse for pyridine than for 2-substituted pyridine derivatives. This shows that testing potential SABRE catalysts on a small set of substrates is insufficient and opportunities for expanding the SABRE substrate scope may be missed. Indeed, the Phox catalyst performs better than the highly optimised (for pyridine) IMes catalyst when considering bulkier substrates. Moreover, attractive features of chelating ligands, such as reliable immobilization and simplification of kinetics to supress non-hyperpolarising exchange pathways, give a promising handle towards the rational design of SABRE catalysts. Altogether, these finding provide a path towards a broader scope of SABRE hyperpolarisation with numerous applications in biomedicine and beyond.[42, 73]

Acknowledgements

There are no conflicts of interests to declare. The authors gratefully acknowledge the support by the National Institute of Biomedical Imaging and Bioengineering of the NIH (R21EB025313). We also gratefully acknowledge funding by the NSF (CHE-1665090) and by Duke University. EYC is grateful for funding support from NSF CHE-1904780, NIH 1R21EB020323 and 1R21CA220137; and DOD CDMRP W81XWH-12-1-0159/BC112431 and W81XWH-15-1-0271. Furthermore, support from the Donors of the American Chemical Society Petroleum Research Fund is gratefully acknowledged.

Author Contributions

J. F. P. C and A. W. J. L. contributed equally, conducted most experimental work, wrote and edited the paper. Z.Z and J. R. L. helped with experimental work and edited the paper. R. L. conducted all ab-initio calculations. R V. S. and E.Y.C. conducted the fluorine hyperpolarisation experiments and edited the paper. V. B. advised the ab-initio calculations and edited/revised the paper, W. S. W. advised the team. S. J. M. advised on chemical design and edited the paper. T. T. advised on data acquisition, wrote, edited and revised the paper.

References

1. R. W. Adams, J. A. Aguilar, K. D. Atkinson, M. J. Cowley, P. I. P. Elliott, S. B. Duckett, G. G. R. Green, I. G. Khazal, J. Lopez-Serrano and D. C. Williamson, *Science*, 2009, **323**, 1708-1711.
2. K. D. Atkinson, M. J. Cowley, P. I. P. Elliott, S. B. Duckett, G. G. R. Green, J. López-Serrano and A. C. Whitwood, *J. Am. Chem. Soc.*, 2009, **131**, 13362-13368.
3. R. W. Adams, S. B. Duckett, R. A. Green, D. C. Williamson and G. G. R. Green, *J. Chem. Phys.*, 2009, **131**.
4. P. Nikolaou, B. M. Goodson and E. Y. Chekmenev, *Chem. Eur. J.*, 2015, **21**, 3156-3166.
5. J.-B. Hövener, A. N. Pravdivtsev, B. Kidd, C. R. Bowers, S. Glöggler, K. V. Kovtunov, M. Plaumann, R. Katz-Brull, K. Buckenmaier, A. Jerschow, F. Reineri, T. Theis, R. V. Shchepin, S. Wagner, N. M. M. Zacharias, P. Bhattacharya and E. Y. Chekmenev, *Angew. Chem. Int. Ed.* , 2018, DOI: 10.1002/anie.201711842.
6. S. B. Duckett and N. J. Wood, *Coordination Chemistry Reviews*, 2008, **252**, 2278-2291.
7. T. Theis, M. L. Truong, A. M. Coffey, R. V. Shchepin, K. W. Waddell, F. Shi, B. M. Goodson, W. S. Warren and E. Y. Chekmenev, *J. Am. Chem. Soc.*, 2015, **137**, 1404-1407.

8. P. J. Rayner, M. J. Burns, A. M. Olaru, P. Norcott, M. Fekete, G. G. R. Green, L. A. R. Highton, R. E. Mewis and S. B. Duckett, *Proc. Natl. Acad. Sci.*, 2017, **114**, E3188-E3194.
9. D. A. Barskiy, R. V. Shchepin, A. M. Coffey, T. Theis, W. S. Warren, B. M. Goodson and E. Y. Chekmenev, *J. Am. Chem. Soc.*, 2016, **138**, 8080-8083.
10. J. F. P. Colell, A. W. J. Logan, Z. Zhou, R. V. Shchepin, D. A. Barskiy, G. X. Ortiz, Q. Wang, S. J. Malcolmson, E. Y. Chekmenev, W. S. Warren and T. Theis, *J. Phys. Chem. C*, 2017, 6626–6634.
11. Z. Zhou, J. Yu, J. F. P. Colell, R. Laasner, A. Logan, D. A. Barskiy, R. V. Shchepin, E. Y. Chekmenev, V. Blum, W. S. Warren and T. Theis, *J. Phys. Chem. Lett.*, 2017, **8**, 3008-3014.
12. A. M. Olaru, T. B. R. Robertson, J. S. Lewis, A. Antony, W. Iali, R. E. Mewis and S. B. Duckett, *ChemistryOpen*, 2018, **7**, 97-105.
13. R. V. Shchepin, B. M. Goodson, T. Theis, W. S. Warren and E. Y. Chekmenev, *Chem. Phys. Chem.*, 2017, **18**, 1961-1965.
14. D. A. Barskiy, R. V. Shchepin, C. P. N. Tanner, J. F. P. Colell, B. M. Goodson, T. Theis, W. S. Warren and E. Y. Chekmenev, *Chem. Phys. Chem.*, 2017, **18**, 1493-1498.
15. V. V. Zhivonitko, I. V. Skovpin and I. V. Koptyug, *Chem. Commun.*, 2015, **51**, 2506-2509.
16. R. E. Mewis, R. A. Green, M. C. R. Cockett, M. J. Cowley, S. B. Duckett, G. G. R. Green, R. O. John, P. J. Rayner and D. C. Williamson, *J. Phys. Chem. B*, 2015, **119**, 1416-1424.
17. J. F. P. Colell, M. Emondts, A. W. J. Logan, K. Shen, J. Bae, R. V. Shchepin, G. X. Ortiz, P. Spannring, Q. Wang, S. J. Malcolmson, E. Y. Chekmenev, M. C. Feiters, F. P. J. T. Rutjes, B. Blümich, T. Theis and W. S. Warren, *J. Am. Chem. Soc.*, 2017, **139**, 7761-7767.
18. S. Lehmkuhl, M. Emondts, L. Schubert, P. Spannring, J. Klankermayer, B. Blümich and P. Schleker, *Chem. Phys. Chem.*, 2017, DOI: 10.1002/cphc.201700750.
19. P. Spannring, I. Reile, M. Emondts, P. P. M. Schleker, N. K. J. Hermkens, N. G. J. van der Zwaluw, B. J. A. van Weerdenburg, P. Tinnemans, M. Tessari, B. Blümich, F. P. J. T. Rutjes and M. C. Feiters, *Chem. Eur. J.*, 2016, **22**, 9277-9282.
20. K. V. Kovtunov, L. M. Kovtunova, M. E. Gemeinhardt, A. V. Bukhtiyarov, J. Gesiorski, V. I. Bukhtiyarov, E. Y. Chekmenev, I. V. Koptyug and B. M. Goodson, *Angew. Chem. Int. Ed.*, 2017, **56**, 10433-10437.
21. F. Shi, P. He, Q. A. Best, K. Groome, M. L. Truong, A. M. Coffey, G. Zimay, R. V. Shchepin, K. W. Waddell, E. Y. Chekmenev and B. M. Goodson, *J. Phys. Chem. C*, 2016, **120**, 12149-12156.
22. M. L. Truong, F. Shi, P. He, B. Yuan, K. N. Plunkett, A. M. Coffey, R. V. Shchepin, D. A. Barskiy, K. V. Kovtunov, I. V. Koptyug, K. W. Waddell, B. M. Goodson and E. Y. Chekmenev, *J. Phys. Chem. B*, 2014, **18** 13882–13889.
23. H. Zeng, J. Xu, M. T. McMahon, J. A. B. Lohman and P. C. M. van Zijl, *J. Magn. Reson.*, 2014, **246**, 119-121.
24. M. Fekete, C. Gibard, G. J. Dear, G. G. R. Green, A. J. J. Hooper, A. D. Roberts, F. Cisnetti and S. B. Duckett, *Dalton Trans.*, 2015, **44**, 7870-7880.
25. J.-B. Hövener, N. Schwaderlapp, R. Borowiak, T. Lickert, S. B. Duckett, R. E. Mewis, R. W. Adams, M. J. Burns, L. A. R. Highton, G. G. R. Green, A. Olaru, J. Hennig and D. von Elverfeldt, *Anal. Chem.*, 2014, **86**, 1767-1774.
26. F. Shi, A. M. Coffey, K. W. Waddell, E. Y. Chekmenev and B. M. Goodson, *J. Phys. Chem. C*, 2015, **119**, 7525–7533.
27. F. Shi, A. M. Coffey, K. W. Waddell, E. Y. Chekmenev and B. M. Goodson, *Angew. Chem. Int. Ed.*, 2014, **53**, 7495–7498.
28. A. M. Olaru, M. J. Burns, G. G. R. Green and S. B. Duckett, *Chem. Sci.*, 2017, **8**, 2257-2266.
29. R. V. Shchepin, D. A. Barskiy, A. M. Coffey, T. Theis, F. Shi, W. S. Warren, B. M. Goodson and E. Y. Chekmenev, *ACS Sensors*, 2016, 640-644.
30. H. Zeng, J. Xu, J. Gillen, M. T. McMahon, D. Artemov, J.-M. Tyburn, J. A. B. Lohman, R. E. Mewis, K. D. Atkinson, G. G. R. Green, S. B. Duckett and P. C. M. van Zijl, *J. Magn. Reson.*, 2013, **237**, 73-78.
31. S. S. Roy, K. M. Appleby, E. J. Fear and S. B. Duckett, *J. Phys. Chem. Lett.*, 2018, **9**, 1112-1117.
32. P. J. Rayner and S. Duckett, *Angew. Chem. Int. Ed.*, 2018, DOI: 10.1002/anie.201710406.
33. K. M. Appleby, R. E. Mewis, A. M. Olaru, G. G. R. Green, I. J. S. Fairlamb and S. B. Duckett, *Chem. Sci.*, 2015, **6**, 3981-3993.
34. R. V. Shchepin, M. L. Truong, T. Theis, A. M. Coffey, F. Shi, K. W. Waddell, W. S. Warren, B. M. Goodson and E. Y. Chekmenev, *J. Phys. Chem. Lett.*, 2015, **6**, 1961-1967.
35. M. J. Cowley, R. W. Adams, K. D. Atkinson, M. C. R. Cockett, S. B. Duckett, G. G. R. Green, J. A. B. Lohman, R. Kerssebaum, D. Kilgour and R. E. Mewis, *J. Am. Chem. Soc.*, 2011, **133**, 6134-6137.
36. X. Bantreil and S. P. Nolan, *Nat. Protoc.*, 2010, **6**, 69-77.
37. L. S. Lloyd, A. Asghar, M. J. Burns, A. Charlton, S. Coombes, M. J. Cowley, G. J. Dear, S. B. Duckett, G. R. Genov, G. G. R. Green, L. A. R. Highton, A. J. J. Hooper, M. Khan, I. G. Khazal, R. J. Lewis, R. E. Mewis, A. D. Roberts and A. J. Ruddlesden, *Catal. Sci. Technol.*, 2014, **4**, 3544-3554.
38. B. J. A. van Weerdenburg, N. Eshuis, M. Tessari, F. P. J. T. Rutjes and M. C. Feiters, *Dalton Trans.*, 2015, 15387-15390.
39. B. J. A. van Weerdenburg, S. Glöggler, N. Eshuis, A. H. J. Engwerda, J. M. M. Smits, R. de Gelder, S. Appelt, S. S. Wymenga, M. Tessari, M. C. Feiters, B. Blümich and F. P. J. T. Rutjes, *Chem. Commun.*, 2013, **49**, 7388.
40. P. J. Rayner, P. Norcott, K. M. Appleby, W. Iali, R. O. John, S. J. Hart, A. C. Whitwood and S. B. Duckett, *Nat. Commun.*, 2018, **9**, 4251.
41. N. Eshuis, R. L. E. G. Aspers, B. J. A. van Weerdenburg, M. C. Feiters, F. P. J. T. Rutjes, S. S. Wijmenga and M. Tessari, *Angew. Chem. Int. Ed.*, 2015, **54**, 14527-14530.
42. N. Eshuis, B. J. A. van Weerdenburg, M. C. Feiters, F. P. J. T. Rutjes, S. S. Wijmenga and M. Tessari, *Angew. Chem. Int. Ed.*, 2015, **54**, 1372-1372.
43. I. Reile, R. L. E. G. Aspers, J.-M. Tyburn, J. G. Kempf, M. C. Feiters, F. P. J. T. Rutjes and M. Tessari, *Angew. Chem. Int. Ed.*, 2017, **56**, 9174-9177.
44. N. Eshuis, N. Hermkens, B. J. A. van Weerdenburg, M. C. Feiters, F. P. J. T. Rutjes, S. S. Wijmenga and M. Tessari, *Journal of the American Chemical Society*, 2014, **136**, 2695-2698.
45. A. J. Holmes, P. J. Rayner, M. J. Cowley, G. G. R. Green, A. C. Whitwood and S. B. Duckett, *Dalton Trans.*, 2015, **44**, 1077-1083.
46. A. J. Ruddlesden, R. E. Mewis, G. G. R. Green, A. C. Whitwood and S. B. Duckett, *Organometallics*, 2015, **34**, 2997-3006.

47. E. B. Ducker, L. T. Kuhn, K. Munnemann and C. Griesinger, *Journal of magnetic resonance*, 2012, **214**, 159-165.
48. C. Mazet, S. P. Smidt, M. Meuwly and A. Pfaltz, *J. Am. Chem. Soc.*, 2004, **126**, 14176-14181.
49. A. Pfaltz, J. Blankenstein, R. Hilgraf, E. Hörmann, S. McIntyre, F. Menges, M. Schönleber, S. P. Smidt, B. Wüstenberg and N. Zimmermann, *Adv. Synth. Catal.*, 2003, **345**, 33-43.
50. B. Wüstenberg and A. Pfaltz, *Adv. Synth. Catal.*, 2008, **350**, 174-178.
51. D. A. Barskiy, A. N. Pravdivtsev, K. L. Ivanov, K. V. Kovtunov and I. V. Koptyug, *Phys. Chem. Chem. Phys.*, 2015, **89**, 89-93.
52. V. Blum, R. Gehrke, F. Hanke, P. Havu, V. Havu, X. Ren, K. Reuter and M. Scheffler, *Comput. Phys. Commun.*, 2009, **180**, 2175-2196.
53. M. Sinstein, C. Scheurer, S. Matera, V. Blum, K. Reuter and H. Oberhofer, *J. Chem. Theory Comput.*, 2017, **13**, 5582-5603.
54. J. P. Perdew, K. Burke and M. Ernzerhof, *Phys. Rev. Lett.*, 1996, **77**, 3865-3868.
55. A. Tkatchenko and M. Scheffler, *Phys. Rev. Lett.*, 2009, **102**.
56. Y. Zhao and D. G. Truhlar, *Theor. Chem. Acc.*, 2007, **120**, 215-241.
57. V. Havu, V. Blum, P. Havu and M. Scheffler, *Journal of Computational Physics*, 2009, **228**, 8367-8379.
58. X. Ren, P. Rinke, V. Blum, J. Wieferink, A. Tkatchenko, A. Sanfilippo, K. Reuter and M. Scheffler, *New Journal of Physics*, 2012, **14**.
59. K. Lejaeghere, G. Bihlmayer, T. Björkman, P. Blaha, S. Blügel, V. Blum, D. Caliste, I. E. Castelli, S. J. Clark, A. Dal Corso, S. de Gironcoli, T. Deutsch, J. K. Dewhurst, I. Di Marco, C. Draxl, M. Dułak, O. Eriksson, J. A. Flores-Livas, K. F. Garrity, L. Genovese, P. Giannozzi, M. Giantomassi, S. Goedecker, X. Gonze, O. Grånäs, E. K. U. Gross, A. Gulans, F. Gygi, D. R. Hamann, P. J. Hasnip, N. A. W. Holzwarth, D. Iuşan, D. B. Jochym, F. Jollet, D. Jones, G. Kresse, K. Koepernik, E. Küçükbenli, Y. O. Kvashnin, I. L. M. Locht, S. Lubeck, M. Marsman, N. Marzari, U. Nitzsche, L. Nordström, T. Ozaki, L. Paulatto, C. J. Pickard, W. Poelmans, M. I. J. Probert, K. Refson, M. Richter, G.-M. Rignanese, S. Saha, M. Scheffler, M. Schlipf, K. Schwarz, S. Sharma, F. Tavazza, P. Thunström, A. Tkatchenko, M. Torrent, D. Vanderbilt, M. J. van Setten, V. Van Speybroeck, J. M. Wills, J. R. Yates, G.-X. Zhang and S. Cottenier, *Science*, 2016, **351**.
60. S. R. Jensen, S. Saha, J. A. Flores-Livas, W. Huhn, V. Blum, S. Goedecker and L. Frediani, *The Journal of Physical Chemistry Letters*, 2017, **8**, 1449-1457.
61. M. Rossi, V. Blum, P. Kupser, G. Von Helden, F. Bierau, K. Pagel, G. Meijer and M. Scheffler, *Journal of Physical Chemistry Letters*, 2010, **1**, 3465-3470.
62. S. Chutia, M. Rossi and V. Blum, *Journal of Physical Chemistry B*, 2012, **116**, 14788-14804.
63. M. Rossi, S. Chutia, M. Scheffler and V. Blum, *The Journal of Physical Chemistry A*, 2014, **118**, 7349-7359.
64. F. Schubert, M. Rossi, C. Baldauf, K. Pagel, S. Warnke, G. von Helden, F. Filsinger, P. Kupser, G. Meijer, M. Salwiczek, B. Koksch, M. Scheffler and V. Blum, *Physical chemistry chemical physics : PCCP*, 2015, **17**, 7373-7385.
65. T. Theis, G. X. Ortiz, A. W. J. Logan, K. E. Claytor, Y. Feng, W. P. Huhn, V. Blum, S. J. Malcolmson, E. Y. Chekmenev, Q. Wang and W. S. Warren, *Sci. Adv.*, 2016, **2**, e1501438-e1501438.
66. C. R. Bowers and D. P. Weitekamp, *J. Am. Chem. Soc.*, 1987, **109**, 5541-5542.
67. A. N. Pravdivtsev, A. V. Yurkovskaya, H.-M. Vieth, K. L. Ivanov and R. Kaptein, *Chem. Phys. Chem*, 2013, **14**, 3327-3331.
68. K. Shen, A. W. J. Logan, J. F. P. Colell, J. Bae, G. X. Ortiz, T. Theis, W. S. Warren, S. J. Malcolmson and Q. Wang, *Angew. Chem. Int. Ed.*, 2017, **56**, 12112-12116.
69. M. L. Truong, T. Theis, A. M. Coffey, R. V. Shchepin, K. W. Waddell, F. Shi, B. M. Goodson, W. S. Warren and E. Y. Chekmenev, *J. Phys. Chem. C*, 2015, **119**, 8786-8797.
70. S. S. Roy, G. Stevanato, P. J. Rayner and S. B. Duckett, *J. Magn. Reson.*, 2017, **285**, 55-60.
71. T. Theis, M. Truong, A. M. Coffey, E. Y. Chekmenev and W. S. Warren, *J. Magn. Reson.*, 2014, **248**, 23-26.
72. M. Fekete, P. J. Rayner, G. G. R. Green and S. B. Duckett, *Magnetic Resonance in Chemistry*, 2017, **55**, 944-957.
73. R. V. Shchepin, D. A. Barskiy, A. M. Coffey, B. M. Goodson and E. Y. Chekmenev, *ChemistrySelect*, 2016, **1**, 2552-2555.

TOC Figure: Phox ligands enable new substrates for SABRE.

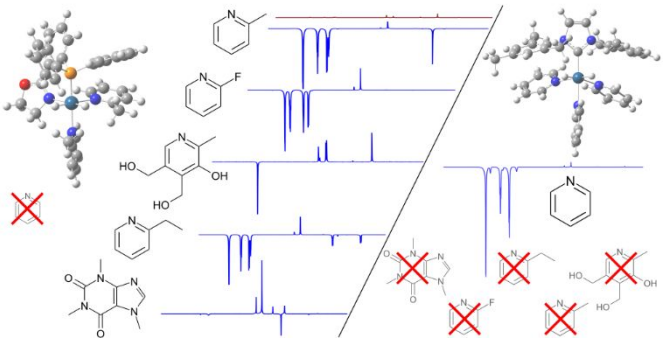

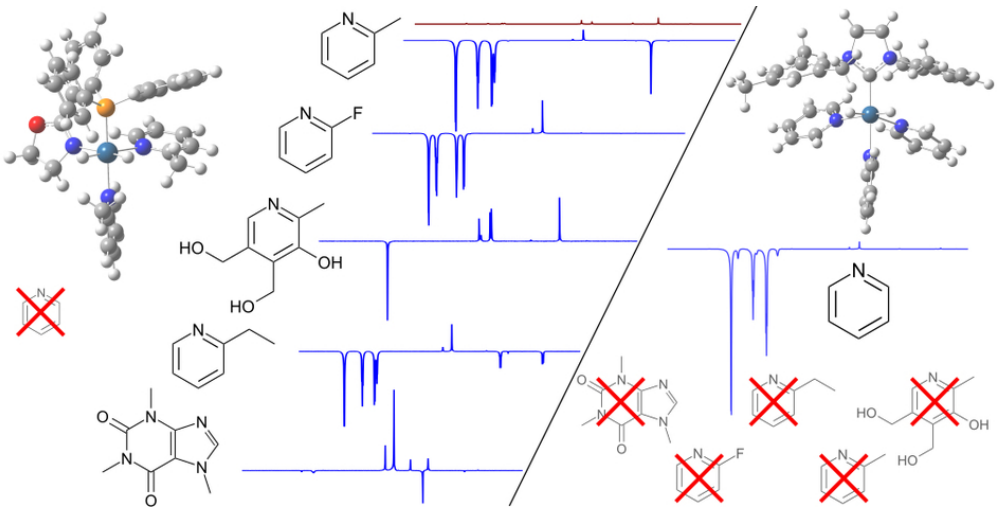

80x40mm (300 x 300 DPI)